

Topological Superconductivity in $\text{Cu}_x\text{Bi}_2\text{Se}_3$

Satoshi Sasaki,¹ M. Kriener,¹ Kouji Segawa,¹ Keiji Yada,² Yukio Tanaka,² Masatoshi Sato,³ and Yoichi Ando^{1,*}

¹*Institute of Scientific and Industrial Research, Osaka University, Ibaraki, Osaka 567-0047, Japan*

²*Department of Applied Physics, Nagoya University, Nagoya 464-8603, Japan*

³*Institute for Solid State Physics, University of Tokyo, Chiba 277-8581, Japan*

(Received 2 August 2011; published 14 November 2011)

A topological superconductor (TSC) is characterized by the topologically protected gapless surface state that is essentially an Andreev bound state consisting of Majorana fermions. While a TSC has not yet been discovered, the doped topological insulator $\text{Cu}_x\text{Bi}_2\text{Se}_3$, which superconducts below ~ 3 K, has been predicted to possess a topological superconducting state. We report that the point-contact spectra on the cleaved surface of superconducting $\text{Cu}_x\text{Bi}_2\text{Se}_3$ present a zero-bias conductance peak (ZBCP) which signifies unconventional superconductivity. Theoretical considerations of all possible superconducting states help us conclude that this ZBCP is due to Majorana fermions and gives evidence for a topological superconductivity in $\text{Cu}_x\text{Bi}_2\text{Se}_3$. In addition, we found an unusual pseudogap that develops below ~ 20 K and coexists with the topological superconducting state.

DOI: 10.1103/PhysRevLett.107.217001

PACS numbers: 74.45.+c, 03.65.Vf, 73.20.At, 74.20.Rp

The recent discovery of topological insulators [1–24] stimulated the search for an even more exotic state of matter, the topological superconductor (TSC) [25–28]. A topological state of matter is characterized by a topological structure of the quantum-mechanical wave function in the Hilbert space. In topological insulators, a nontrivial Z_2 topology of the bulk valence band leads to the emergence of Dirac fermions on the surface [22,23]. Similarly, in TSCs nontrivial Z or Z_2 topologies of the superconducting (SC) states lead to the appearance of Majorana fermions on the surface [25–27]. Majorana fermions are peculiar in that the particles are their own antiparticles, and they were originally conceived as mysterious neutrinos [29]. Currently their realization in condensed matter is of significant interest because of their novelty as well as the potential for quantum computing [29].

The $\text{Cu}_x\text{Bi}_2\text{Se}_3$ superconductor [30–33] is a prime candidate of the TSC because of its peculiar band structure and strong spin-orbit coupling [34]. In this material, Cu atoms are intercalated into the layered topological insulator Bi_2Se_3 and the SC state appears for the Cu concentration x of about 0.2–0.5, which causes electron doping with the density of $\sim 10^{20} \text{ cm}^{-3}$. This material has not been well studied because of the difficulty in preparing high-quality samples [30,31] but a recent breakthrough in the synthesis of $\text{Cu}_x\text{Bi}_2\text{Se}_3$ by using electrochemistry [32,33] made it possible to prepare reliable junctions and perform a conductance spectroscopy in the superconducting state.

In the present work, we employed the so-called “soft” point-contact technique [35]: The contacts were prepared at room temperature in ambient atmosphere by putting a tiny ($\sim 20 \mu\text{m}$) drop of silver paste on the cleaved (111) surface of a $\text{Cu}_x\text{Bi}_2\text{Se}_3$ single crystal below a $30\text{-}\mu\text{m}$ -diameter gold wire [Figs. 1(a) and 1(b)]. In this

type of junction, ballistic transport occurs sporadically through parallel nanometer-scale channels formed between individual grains in the silver paste and the sample surface [see Figs. 1(c) and 1(d) and Ref. [36]]. The dI/dV spectra were measured with a lock-in technique by sweeping a dc current that is superimposed with a small-amplitude ac current [$1.35 \mu\text{A}$ (rms), corresponding to 0.5 A/cm^2]. We used a quasi-four-probe configuration, in which the

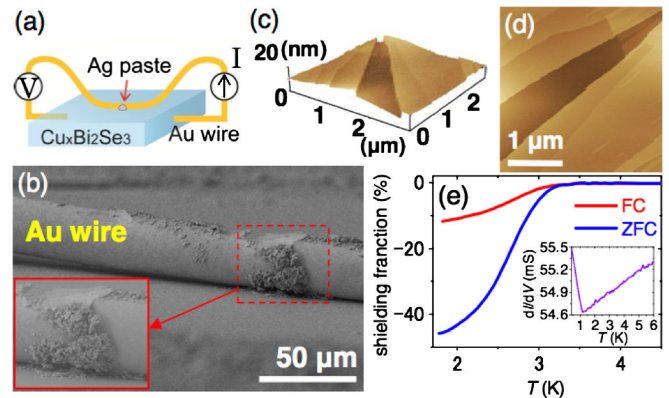


FIG. 1 (color online). Point-contact experiment and the sample. (a) Sketch of the soft point contact and the measurement circuit. (b) Scanning-electron-microscope picture of the actual sample; inset magnifies the silver-paste spot where the point contact is formed. (c) 3D presentation of nanometer-scale terraces on a typical cleaved surface of $\text{Cu}_x\text{Bi}_2\text{Se}_3$ seen by an atomic-force microscope. Typical terrace width is $0.5 \mu\text{m}$. (d) A false color mapping of (c). (e) SQUID data for the SC transition in the sample ($x = 0.3$) used for the point-contact measurements shown in Fig. 2. Both the zero-field-cooled (ZFC) and the field-cooled (FC) data measured in 0.2 mT are shown, and the former gives the SC shielding fraction of 46%. Inset shows the temperature dependence of the zero-bias differential conductance of the point contact reported in Fig. 2.

current was applied between a contact pad and the gold wire, and the voltage between the wire and another contact pad was measured [Fig. 1(a)]. The Quantum Design PPMS was used for cooling the samples down to 0.35 K and applying the magnetic field up to 9 T.

A set of point-contact data taken on a $\text{Cu}_x\text{Bi}_2\text{Se}_3$ sample with the bulk onset $T_c = 3.2$ K is shown in Fig. 2, where one can see that a pronounced zero-bias conductance peak (ZBCP) develops at low temperature [36]. The inset of Fig. 1(e) shows the temperature dependence of the zero-bias conductance, which indicates that this peak appears below 1.2 K [36]. We note that essentially the same ZBCP data have been obtained on another sample (see Fig. S2 of Ref. [36]).

Since heating effects can cause a spurious ZBCP [37], it is important to elucidate that it is not the case here. It was argued by Sheet *et al.* [37] that in samples with a large normal-state resistivity when the point contact is in the thermal regime, a spurious ZBCP could show up if the increase in the bias voltage causes the local current to exceed the critical current, which leads to a voltage-dependent decrease in the differential conductivity. If this is the case, the conductivity at zero bias (which is always measured below the critical current) should *not* change with a weak magnetic field; the role of the magnetic field in this case is primarily to reduce the critical current, so the width of the spurious ZBCP would become narrower, but the height at $V = 0$ should be mostly unchanged as long as the superconductor is in the zero-resistivity state. In the magnetic-field dependence of our spectra shown in Fig. 2(c), by contrast, the ZBCP is strongly suppressed with a modest magnetic field while its width is little affected, which clearly speaks against the heating origin of the ZBCP. (The magnetic field was applied perpendicular to the cleaved surface.) Another well-known signature of the heating effect is a sharp, spikelike dip at energies much larger than the gap [35,37], which is caused by the local transition to normal state; in fact, when we made the point contact on a disordered surface, we observed a widening of the peak and a lot of sharp dips at relatively high energies, which are obviously caused by the heating [36]. In contrast, the data shown in Fig. 2 are free from such

features, which corroborates the intrinsic nature of the ZBCP. Therefore, one can safely conclude that the ZBCP observed here is not due to the heating effects and is intrinsic.

One should also keep in mind that, even when the ZBCP is intrinsic, it can be caused by several mechanisms in point contacts [38]: conventional Andreev reflection [39,40], reflectionless tunneling [41–43], magnetic scattering [44,45], and the unconventional Andreev bound state (ABS) [38,40]. In this respect, it is important to notice that the ZBCP shown in Fig. 2 is accompanied by pronounced dips on its sides and the peak does not split into two even at the lowest temperature (0.35 K). These features are clearly at odds with the Blonder-Tinkham-Klapwijk (BTK) theory for conventional Andreev reflection [39]. Also, the reflectionless tunneling and the magnetic scattering are obviously irrelevant, because the former is suppressed by a very small magnetic field of less than 0.1 T [46] and the latter presents a peak splitting in magnetic fields [47]. Hence, one can conclude that the ZBCP observed here is a manifestation of the ABS [38].

Previously, it was inferred [32] from the specific-heat data that the superconducting gap of $\text{Cu}_x\text{Bi}_2\text{Se}_3$ at $T = 0$ K, $\Delta(0)$, would be about 0.7 meV. In Fig. 2, one can see that the minima in the pronounced dips are located at $\sim \pm 0.6$ meV at 0.35 K; since the ZBCP due to the ABS is usually accompanied by dips near the gap energy [38], the energy scale of the dip is assuring.

Given that the observed ZBCP is intrinsic and is due to the ABS, it is important to understand its concrete origin. The ABS is caused by the interference of the SC wave function at the surface, and it is a signature of unconventional superconductivity [38]. Its occurrence is determined by the symmetry of the SC state, which in turn is determined by the symmetry of the Hamiltonian and the pairing mechanism. Also, it has been elucidated that Majorana fermions reside in an ABS when it is spin nondegenerate [48]. Hence, we examined all possible SC states in $\text{Cu}_x\text{Bi}_2\text{Se}_3$ and the nature of the ABS to elucidate whether the observed ZBCP is due to Majorana fermions. The microscopic model to describe the band structure of $\text{Cu}_x\text{Bi}_2\text{Se}_3$ has already been developed [34,49–51], and

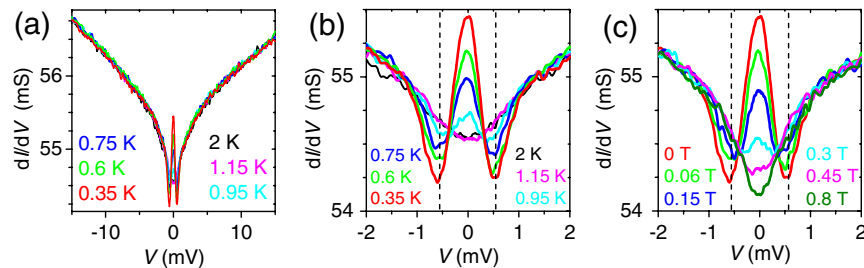


FIG. 2 (color online). Zero-bias conductance peak. (a) Point-contact spectra (dI/dV vs bias voltage) of $\text{Cu}_x\text{Bi}_2\text{Se}_3$ with $x = 0.3$ for 0.35–2 K measured in 0 T for a wide energy window. (b) A narrower window of (a). (c) The spectra at 0.35 K measured in perpendicular magnetic fields of 0–0.8 T. The vertical dashed lines in (b) and (c) indicate the energy position of the dips.

it was shown [34] that, if both short- and long-range interactions are considered, the symmetry of the Hamiltonian allows four different types of the SC gap function, Δ_1 to Δ_4 [36], with three of them being unconventional. Following Ref. [51], we have theoretically calculated the spectral functions of the bulk and the surface as well as the local density of states (LDOS) for all possible gap functions (see Ref. [36] for details), similar to those done in Refs. [52,53].

First, the conventional even-parity SC state Δ_1 was found to give no two-dimensional (2D) ABS [36]. While in this case the surface could become a 2D TSC due to the proximity effect as proposed by Fu and Kane [28], the surface of a three-dimensional (3D) superconductor is continuously connected and has no topological edge; hence, the one-dimensional Majorana fermions that might appear at the edge of a 2D TSC [28] would not exist in the present case.

Among the remaining three possible SC states that are all unconventional, the fully-gapped, odd-parity SC state Δ_2 gives rise to 2D helical Majorana fermions as the ABS. However, because of the Dirac-like dispersion of this ABS, the surface LDOS tends to have a minimum at zero energy [36], which does not agree well with our data; nevertheless, it was very recently proposed that the ZBCP could appear even in this fully gapped state due to a peculiar “twisting” of the ABS dispersion [54]. In the case of the other two odd-parity SC states, Δ_3 and Δ_4 , both of which have two point nodes, a single ZBCP naturally shows up in the surface LDOS [Figs. 3(a)–3(c)]; this is because the point nodes lead to a partially flat dispersion of the helical Majorana fermions, concentrating the LDOS near zero energy. Therefore, it is most likely that the observed ZBCP signifies 2D Majorana fermions due to the odd-parity bulk SC state, although it is difficult to determine the exact pairing state from the three possibilities at this stage. The fact that the ZBCP is strongly suppressed with a modest magnetic field [Fig. 2(c)] supports this conclusion, because the helical Majorana fermions are naturally suppressed as the time-reversal symmetry is broken with the

magnetic field. Note that, while there are nanometer-scale terraces on the cleaved surface (Figs. 1(c) and 1(d) and Ref. [36]), electron transmissions in the in-plane directions through the side walls of the terraces are much less likely to take place compared to the transmissions in the out-of-plane direction, because the typical terrace height (< 10 nm) is much smaller than the typical Ag grain size of 50 nm [36]. Therefore, our data are expected to reflect mostly the ABS on the (111) surface.

We now discuss the topological nature of the possible SC states Δ_3 and Δ_4 . The presence of the point nodes might seem to preclude the topological superconductivity, which is usually considered to require a full gap. However, for the Δ_3 and Δ_4 states one can define a nontrivial topological invariant, “mod-2 winding number,” which is immune to weak perturbations and assures that the Δ_3 and Δ_4 states are robustly topological [36]. In fact, a time-reversal-invariant SC state with a pair of point nodes is adiabatically connected to a fully gapped state in the “mod-2 winding number” topological class, and having an odd parity is sufficient for this case to become topologically nontrivial [36].

Previously, we reported that the specific-heat data was most consistent with a fully-gapped SC state [32]. It is fair to note, however, that the entropy contribution of the quasiparticles excited near the point node of a 3D SC state is very small and, indeed, the T^3 dependence of the specific heat expected for point nodes is difficult to be distinguished [55], particularly in inhomogeneous samples. Therefore, the Δ_3 or Δ_4 state with point nodes does not necessarily contradict the existing specific-heat data.

An interesting and unexpected feature in our data is that a pseudogap develops below ~ 20 K [Fig. 4(a)]. As shown in Figs. 4(b)–4(g), this pseudogap appears to be enhanced by the magnetic field, and it is most pronounced at 0.35 K in high magnetic fields. This pseudogap coexists with the superconductivity below the upper critical field H_{c2} [56] and may give us a clue to understanding the pairing mechanism in $\text{Cu}_x\text{Bi}_2\text{Se}_3$. Finally, how the spectra change with

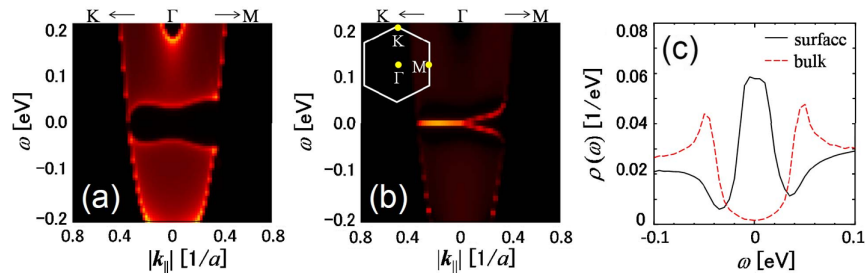


FIG. 3 (color online). Model calculations of the topological band structure in the superconducting state of $\text{Cu}_x\text{Bi}_2\text{Se}_3$. Theoretically calculated spectral functions $A(\mathbf{k}, \omega)$ of the bulk (a) and the surface on the xy plane (b) in Γ - M and Γ - K directions in the surface Brillouin zone shown in the inset of (b), as well as the LDOS (c), in the superconducting state for the topological gap function Δ_4 ($\Delta_{\parallel}^{12} = \Delta_{\parallel}^{21} = -\Delta_{\parallel}^{21} = -\Delta_{\parallel}^{12}$); the model Hamiltonian and the band parameters used are described in detail in Ref. [36]. The false color mappings of $A(\mathbf{k}, \omega)$ in (a) and (b) are in arbitrary units. $\Delta(0)$ was set to be 0.05 eV for the convenience of the calculations.

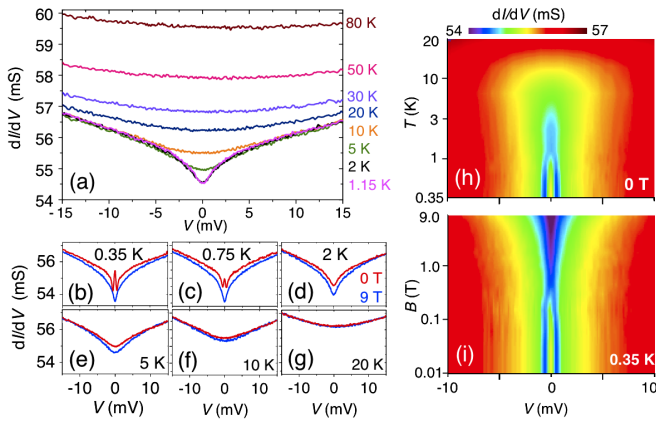


FIG. 4 (color online). Pseudogap in $\text{Cu}_x\text{Bi}_2\text{Se}_3$. (a) dI/dV vs bias voltage for 1.15–80 K measured in 0 T. (b)–(g) Comparisons of the spectra in 0 and 9 T. At low temperature below ~ 20 K, the spectra in 9 T show smaller dI/dV near zero bias compared to that at 0 T, indicating that the pseudogap deepens with the magnetic field. (h),(i) False color mappings of dI/dV in the bias-voltage vs temperature plane in 0 T (h) and in the bias-voltage vs magnetic-field plane at 0.35 K (i), summarizing how the spectra change with temperature and magnetic field; note that the vertical axes are in logarithmic scales in both (h) and (i).

temperature and magnetic field is summarized in false color mappings shown in Figs. 4(h) and 4(i).

As is clear from the above discussions, one can conclude that the ZBCP in $\text{Cu}_x\text{Bi}_2\text{Se}_3$ signifies an ABS consisting of 2D Majorana fermions and that $\text{Cu}_x\text{Bi}_2\text{Se}_3$ is hosting a topological superconductivity. It is therefore an urgent task to determine the exact pairing symmetry in $\text{Cu}_x\text{Bi}_2\text{Se}_3$. Regarding the Majorana physics, an interesting question is the existence of the Majorana zero mode in the vortex core [57]. The 2D Majorana fermions living on the surface of a 3D TSC are different from the non-Abelian Majorana fermions of a 2D TSC proposed for topological quantum computing [22,28], but establishing a general understanding of Majorana fermions is important for both fundamental physics and future information technologies.

In summary, our point-contact spectroscopy of the $\text{Cu}_x\text{Bi}_2\text{Se}_3$ superconductor found an unusual pseudogap below ~ 20 K and a pronounced ZBCP in the SC state. The latter signifies an unconventional SC state that can only be topological in $\text{Cu}_x\text{Bi}_2\text{Se}_3$, and therefore our observation gives evidence for a topological superconductivity in this material. One can fully expect that $\text{Cu}_x\text{Bi}_2\text{Se}_3$ as the first concrete example of a TSC will greatly help advance our understanding of topological states of matter and associated exotic quasiparticles.

We thank L. Fu, A. Furusaki, and S. Onoda for useful discussions, and K. Matsumoto and S. Wada for their help in the experiment. This work was supported by JSPS (NEXT Program), MEXT (Innovative Area “Topological Quantum Phenomena” KAKENHI), and AFOSR (AOARD 10-4103).

*y_ando@sanken.osaka-u.ac.jp

- [1] C.L. Kane and E.J. Mele, *Phys. Rev. Lett.* **95**, 146802 (2005).
- [2] B.A. Bernevig, T.L. Hughes, and S.-C. Zhang, *Science* **314**, 1757 (2006).
- [3] M. König, S. Wiedmann, C. Brüne, A. Roth, H. Buhmann, L.W. Molenkamp, X.-L. Qi, and S.-C. Zhang, *Science* **318**, 766 (2007).
- [4] L. Fu, C.L. Kane, and E.J. Mele, *Phys. Rev. Lett.* **98**, 106803 (2007).
- [5] J.E. Moore and L. Balents, *Phys. Rev. B* **75**, 121306(R) (2007).
- [6] R. Roy, *Phys. Rev. B* **79**, 195322 (2009).
- [7] X.-L. Qi, T.L. Hughes, and S.-C. Zhang, *Phys. Rev. B* **78**, 195424 (2008).
- [8] L. Fu and C.L. Kane, *Phys. Rev. B* **76**, 045302 (2007).
- [9] D. Hsieh, D. Qian, L. Wray, Y. Xia, Y.S. Hor, R.J. Cava, and M.Z. Hasan, *Nature (London)* **452**, 970 (2008).
- [10] A.A. Taskin and Y. Ando, *Phys. Rev. B* **80**, 085303 (2009).
- [11] A. Nishide, A.A. Taskin, Y. Takeichi, T. Okuda, A. Kakizaki, T. Hirahara, K. Nakatsuji, F. Komori, Y. Ando, and I. Matsuda, *Phys. Rev. B* **81**, 041309(R) (2010).
- [12] Y.L. Chen, J.G. Analytis, J.-H. Chu, Z.K. Liu, S.-K. Mo, X.L. Qi, H.J. Zhang, D.H. Lu, X. Dai, Z. Fang, S.C. Zhang, I.R. Fisher, Z. Hussain, and Z.-X. Shen, *Science* **325**, 178 (2009).
- [13] D. Hsieh, Y. Xia, D. Qian, L. Wray, F. Meier, J.H. Dil, J. Osterwalder, L. Patthey, A.V. Fedorov, H. Lin, A. Bansil, D. Grauer, Y.S. Hor, R.J. Cava, and M.Z. Hasan, *Phys. Rev. Lett.* **103**, 146401 (2009).
- [14] Y. Xia, D. Qian, D. Hsieh, L. Wray, A. Pal, H. Lin, A. Bansil, D. Grauer, Y.S. Hor, R.J. Cava, and M.Z. Hasan, *Nature Phys.* **5**, 398 (2009).
- [15] T. Sato, K. Segawa, H. Guo, K. Sugawara, S. Souma, T. Takahashi, and Y. Ando, *Phys. Rev. Lett.* **105**, 136802 (2010).
- [16] K. Kuroda, M. Ye, A. Kimura, S.V. Ereemeev, E.E. Krasovskii, E.V. Chulkov, Y. Ueda, K. Miyamoto, T. Okuda, K. Shimada, H. Namatame, and M. Taniguchi, *Phys. Rev. Lett.* **105**, 146801 (2010).
- [17] Y.L. Chen, Z.K. Liu, J.G. Analytis, J.-H. Chu, H.J. Zhang, B.H. Yan, S.-K. Mo, R.G. Moore, D.H. Lu, I.R. Fisher, S.-C. Zhang, Z. Hussain, and Z.-X. Shen, *Phys. Rev. Lett.* **105**, 266401 (2010).
- [18] Z. Ren, A.A. Taskin, S. Sasaki, K. Segawa, and Y. Ando, *Phys. Rev. B* **82**, 241306(R) (2010).
- [19] S.Y. Xu, L.A. Wray, Y. Xia, R. Shankar, A. Petersen, A. Fedorov, H. Lin, A. Bansil, Y.S. Hor, D. Grauer, R.J. Cava, and M.Z. Hasan, *arXiv:1007.5111v1*.
- [20] J. Xiong, A.C. Petersen, Dongxia Qu, R.J. Cava, and N.P. Ong, *arXiv:1101.1315*.
- [21] A.A. Taskin, Z. Ren, S. Sasaki, K. Segawa, and Y. Ando, *Phys. Rev. Lett.* **107**, 016801 (2011).
- [22] M.Z. Hasan and C.L. Kane, *Rev. Mod. Phys.* **82**, 3045 (2010).
- [23] J.E. Moore, *Nature (London)* **464**, 194 (2010).
- [24] X.-L. Wang, S.X. Dou, and C. Zhang, *NPG Asia Mater.* **2**, 31 (2010).

- [25] X.-L. Qi and S.-C. Zhang, *Rev. Mod. Phys.* **83**, 1057 (2011).
- [26] A. P. Schnyder, S. Ryu, A. Furusaki, and A. W. W. Ludwig, *Phys. Rev. B* **78**, 195125 (2008).
- [27] M. Sato, *Phys. Rev. B* **81**, 220504(R) (2010).
- [28] L. Fu and C. L. Kane, *Phys. Rev. Lett.* **100**, 096407 (2008).
- [29] F. Wilczek, *Nature Phys.* **5**, 614 (2009).
- [30] Y. S. Hor, A. J. Williams, J. G. Checkelsky, P. Roushan, J. Seo, Q. Xu, H. W. Zandbergen, A. Yazdani, N. P. Ong, and R. J. Cava, *Phys. Rev. Lett.* **104**, 057001 (2010).
- [31] L. A. Wray, S.-Y. Xu, Y. Xia, Y. S. Hor, D. Qian, A. V. Fedorov, H. Lin, A. Bansil, R. J. Cava, and M. Z. Hasan, *Nature Phys.* **6**, 855 (2010).
- [32] M. Kriener, K. Segawa, Z. Ren, S. Sasaki, and Y. Ando, *Phys. Rev. Lett.* **106**, 127004 (2011).
- [33] M. Kriener, K. Segawa, Z. Ren, S. Sasaki, S. Wada, S. Kuwabata, and Y. Ando, *Phys. Rev. B* **84**, 054513 (2011).
- [34] L. Fu and E. Berg, *Phys. Rev. Lett.* **105**, 097001 (2010).
- [35] D. Daghero and R. S. Gonnelli, *Supercond. Sci. Technol.* **23**, 043001 (2010).
- [36] See Supplemental Material at <http://link.aps.org/supplemental/10.1103/PhysRevLett.107.217001> for supplemental data and discussions.
- [37] G. Sheet, S. Mukhopadhyay, and P. Raychaudhuri, *Phys. Rev. B* **69**, 134507 (2004).
- [38] S. Kashiwaya and Y. Tanaka, *Rep. Prog. Phys.* **63**, 1641 (2000); Y. Tanaka and S. Kashiwaya, *Phys. Rev. Lett.* **74**, 3451 (1995).
- [39] G. E. Blonder, M. Tinkham, and T. M. Klapwijk, *Phys. Rev. B* **25**, 4515 (1982).
- [40] G. Deutscher, *Rev. Mod. Phys.* **77**, 109 (2005).
- [41] A. Kastalsky, A. W. Kleinsasser, L. H. Greene, R. Bhat, F. P. Milliken, and J. P. Harbison, *Phys. Rev. Lett.* **67**, 3026 (1991).
- [42] C. W. J. Beenakker, *Phys. Rev. B* **46**, 12 841 (1992); I. K. Marmorkos, C. W. J. Beenakker, and R. A. Jalabert, *Phys. Rev. B* **48**, 2811 (1993).
- [43] B. J. van Wees, P. de Vries, P. Magnée, and T. M. Klapwijk, *Phys. Rev. Lett.* **69**, 510 (1992).
- [44] J. A. Appelbaum, *Phys. Rev.* **154**, 633 (1967).
- [45] L. Y. L. Shen and J. M. Rowell, *Phys. Rev.* **165**, 566 (1968).
- [46] The footprint of our point contact is $\sim 20 \mu\text{m}$, which is larger than the dephasing length L_ϕ of $\sim 1 \mu\text{m}$ in Ag below 1 K [P. McConville and N. O. Birge, *Phys. Rev. B* **47**, 16667 (1993)]. This means that L_ϕ governs the reflectionless tunneling [42] which would be suppressed with ~ 0.7 mT.
- [47] The g factor of Bi_2Se_3 is as large as 32 for $H \parallel C_3$ [H. Köhler and E. Wöchner, *Phys. Status Solidi B* **67**, 665 (1975)], which suggests that the Zeeman splitting for $S = 1/2$ in 0.1 T would be ~ 0.2 meV. This should be observable if the magnetic scattering is relevant.
- [48] J. Linder, Y. Tanaka, T. Yokoyama, A. Sudbø, and N. Nagaosa, *Phys. Rev. Lett.* **104**, 067001 (2010).
- [49] H. Zhang, C.-X. Liu, X.-L. Qi, X. Dai, Z. Fang, and S. C. Zhang, *Nature Phys.* **5**, 438 (2009).
- [50] C.-X. Liu, X.-L. Qi, H. Zhang, X. Dai, Z. Fang, and S.-C. Zhang, *Phys. Rev. B* **82**, 045122 (2010).
- [51] L. Hao and T. K. Lee, *Phys. Rev. B* **83**, 134516 (2011).
- [52] A. P. Schnyder, P. M. R. Brydon, D. Manske, and C. Timm, *Phys. Rev. B* **82**, 184508 (2010).
- [53] K. Yada, M. Sato, Y. Tanaka, and T. Yokoyama, *Phys. Rev. B* **83**, 064505 (2011).
- [54] T. Hsieh and L. Fu, [arXiv:1109.3464](https://arxiv.org/abs/1109.3464).
- [55] H. R. Ott, H. Rudigier, T. M. Rice, K. Ueda, Z. Fisk, and J. L. Smith, *Phys. Rev. Lett.* **52**, 1915 (1984).
- [56] With resistivity measurements, we confirmed that the SC state is completely suppressed with the perpendicular magnetic field of 3 T (with the midpoint H_{c2} of 1.7 T) at 0.35 K, consistent with the reported $H_{c2}(T)$ diagram [32].
- [57] P. Hosur, P. Ghaemi, R. S. K. Mong, and A. Vishwanath, *Phys. Rev. Lett.* **107**, 097001 (2011).